Journal of the European Ceramic Society **19** (1999) 2317–2323

PII: S0955-2219(99)00093-X
0955-2219/99/$ - see front matter

Compression Creep Behaviour of Precursor-derived Si–C–N Ceramics

Günter Thurn,[ab]* Jérôme Canel,[ab] Joachim Bill[ab] and Fritz Aldinger[ab]

[a]Max-Planck-Institut für Metallforschung, Germany
[b]Institut für Nichtmetallische Anorganische Materialien, Universität Stuttgart, Pulvermetallurgisches Laboratorium, Heisenbergstrasse 5, 70569 Stuttgart, Germany

Abstract

The creep behaviour of Si–C–N materials derived from polyvinylsilazane (PVS) and polyhydridomethylsilazane (PHMS) precursors was investigated in the temperature range between 1200 and 1550°C at compressive stresses between 30 and 250 MPa in air. Both materials show very similar creep behaviour. Decreasing strain rates with time were observed. Even after 4×10^6 s creep deformation, stationary creep was not observed. Temperature dependence of the creep behaviour of such materials is very low. Dense passivating oxide layers were found on the surface of creep specimens tested in the temperature range up to 1500°C. At 1550°C active oxidation was observed. © *1999 Elsevier Science Ltd. All rights reserved.*

Keywords: creep, precursors-organic, Si–C–N ceramics, mechanical properties, oxidation.

1 Introduction

The condensation of Si–(B–)C–N-based preceramic compounds by thermolysis is known to build up amorphous covalent bonded inorganic solids.[1–3] The structure of amorphous Si–C–N is very similar to those of crystalline phases of the constituent elements.[4–7] It consists of SiX_4 tetrahedra (X = C and/or N) forming three-dimensional networks in which each tetrahedron is attached to four neighbouring tetrahedra. Whereas in the crystalline state the SiX_4 tetrahedral network is periodic, it lacks symmetry or long-range periodicity in the amorphous state and has some molar-free volume associated with it to accommodate the structural imperfection. The amorphous state of such materials thus is similar to a great extent to the so-called random network model, first proposed by Zachariasen,[8] accepted as the best description of the structure of vitreous or fused silica. Due to these structural similarities these materials can be considered as glass-type materials and their plastic flow as viscous flow. Because of their covalent amorphous structure these materials reveal quite interesting mechanical high-temperature properties as has been shown in some preliminary investigations.[6,9–13]

2 Experimental Procedure

To analyse the compression creep behaviour of polymer-derived ceramics, two types of materials were prepared: one material was derived from a polyvinylsilazane (PVS) precursor (VT50, Hoechst AG, Germany), and the other material from a polyhydridomethylsilazane (PHMS) precursor (NCP 200, Nichimen Corp., Japan). The structural units of the precursors and the composition of the ceramics obtained by thermolysis within the isothermal section of the phase-diagram valid up to 1438°C are shown in Fig. 1. The chemical composition of the PVS-derived ceramics was $SiC_{1.6}N_{1.3}$. The PHMS-derived material had the composition $SiC_{0.6}N$. Both materials were produced by plastic forming of crosslinked and ground powder. Both types of powder compacts were thermolysed at 1050°C. The porosity of the PVS- and PHMS-derived material were 4 and 14%, respectively. Details of sample preparation are presented elsewhere.[14]

The specimens for the creep experiments were cut and ground to a height of 7·5 mm with a cross sectional area of $1{\cdot}5\times1{\cdot}5\,mm^2$. A square cross-sectional

*To whom correspondence should be addressed.

area was chosen to facilitate the preparation of the specimens. The creep tests were performed in air at temperatures between 1200 and 1550°C. The temperature was measured with a PtRh(10)/Pt thermocouple which was placed 2 mm from the specimen surface. The load was applied by a spiral spring which was preloaded by a spindle. The compression of the spiral spring was measured by a linear potentiometer and the load of the specimen was calculated from the elongation with an accuracy of ±1 N. The strain of the specimen was calculated from the displacement of the load pads: two SiC scanning pins connected the upper load pad with the housing of an inductive strain gage which was placed under the specimen outside the furnace in the cold part of the testing machine. The displacement between the upper and the lower load pad was measured with a third scanning pin which connected the sensor of the strain gage with the lower load pad.

Since oxidation of the test samples was observed at intermediate temperatures before a protective layer of silica was formed at higher temperatures, the samples were heated quickly to the testing temperature by using the maximum power of the furnace in order to avoid oxidation. The heating ramp for tests at 1550°C is shown in Fig. 2.

During the heating a clamping force of about 2 N was applied to the specimens. After the test temperature was reached, a waiting period of 30 min was necessary to get the strain measurement system into thermal balance. After the waiting period the testing stress was applied within 30 s. The strain measurement started after the testing stress was reached. A schematic diagram of the experimental procedure is presented in Fig. 3.

3 Results

3.1 Creep resistance

For the analysis of the creep results the Norton power-law relation

$$\dot{\varepsilon} = A \cdot t^{-c} \cdot \sigma^{n} \cdot \exp\left(\frac{-Q}{R \cdot T}\right)$$

was taken, where A is a constant, t the time, c the time exponent, σ is the creep stress, n the stress exponent, Q the activation energy, R the gas constant, and T the temperature in K.

Figure 4 shows creep curves of the PVS-derived material tested under 100 MPa compression stress at 1400, 1500 and 1550°C. The strain rates decrease

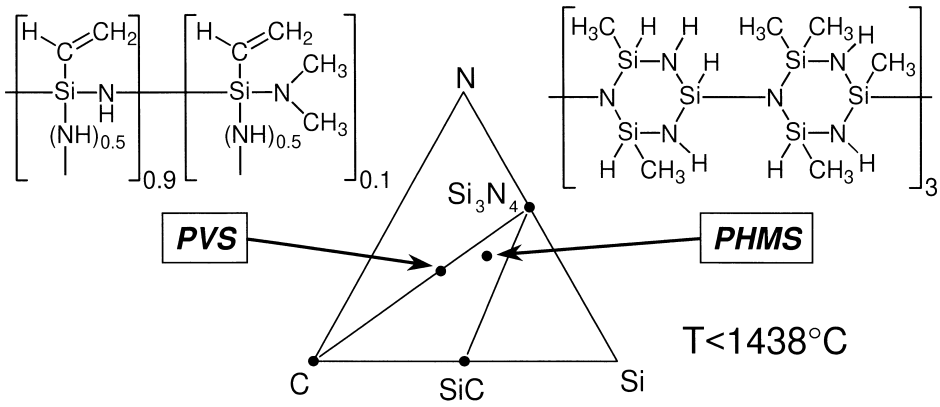

Fig. 1. Structure units of the precursors and chemical composition of the ceramics obtained by pyrolysis within the isothermal section of the ternary system Si–C–N below 1438°C.

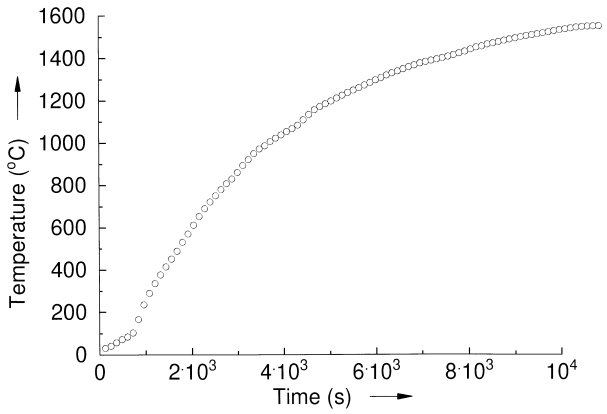

Fig. 2. Heating ramp for a compression creep test at 1550°C.

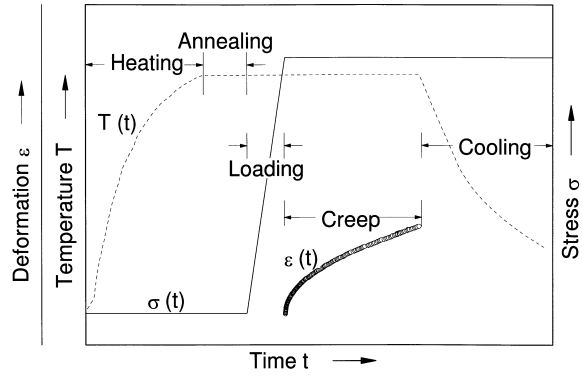

Fig. 3. Experimental procedure of the compression creep test.

with time in very much the same way. Even after 4×10^6 s of creep deformation at 1400°C, stationary creep is not observed. The slope of the curves increases with time. After 100 h a time exponent of $c = 1.1$ was calculated. The increase of the strain rate after approximately 2×10^5 s during the test at 1500°C is an artefact due to an increase of the room temperature in the testing laboratory during the weekend. The opposite effect with a decrease of strain rate is observed after 4×10^5 s when the laboratory was cooled down again. The temperature dependence of strain rates can be described by the apparent activation energy Q which was calculated from the strain rates at $3{\cdot}6\times10^5$ s creep deformation. The apparent activation energy was $Q = 260$ kJ mol^{-1} temperature range between 1400 and 1500°C. Between 1500 and 1550°C the strain rates do not change. Figure 5 shows the influence of compression stress on the strain rate. From the strain rate after $3{\cdot}6\times10^5$ s creep deformation an apparent stress exponent of $n = 0{\cdot}7$ was determined.

The creep results of the PHMS-derived material at a compression stress of 100 MPa and different temperatures are shown in Fig. 6. The strain rates decrease with time. The evolution of the time exponent was very similar to that of the PVS-derived material. The exponent increased after approx. 10 000 s. At $3{\cdot}6\times10^5$ s of creep deformation the time exponents were between $c = 0{\cdot}8$ and 1·0 with the lower exponents in general observed at lower temperatures. In the temperature range between 1200 and 1400°C, the differences between the strain rates are within the experimental scatter of the results. The apparent activation energy therefore seems to be zero. Between 1400 and 1500°C the strain rate increased. At $3{\cdot}6\times10^5$ s creep deformation an activation energy of 250 kJ mol^{-1} was determined. Increasing the temperature to 1550°C, the creep rate decreased with increasing temperature. The stress dependence of the strain rates can be obtained from the curves in Fig. 7. An evaluation of the creep rates at $3{\cdot}6\times10^5$ s creep deformation revealed increasing apparent stress exponents with stress. It increased from $n = 0{\cdot}24$ for stresses between 30 and 100 MPa to $n = 1{\cdot}35$ between 100 and 200 MPa.

The creep resistance can be improved by a heat treatment prior to testing. Figure 8 shows a comparison

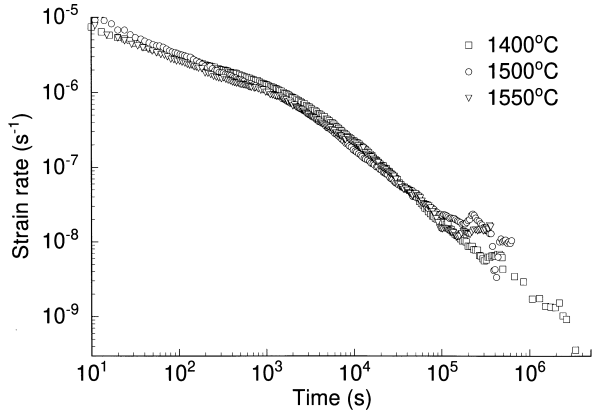

Fig. 4. Temperature dependence of the strain rates at a compression stress of 100 MPa for the PVS-derived material.

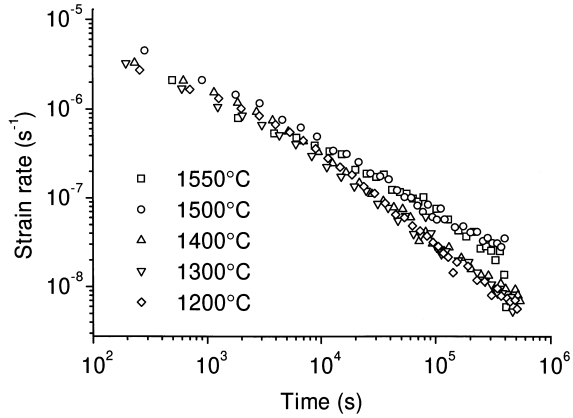

Fig. 6. Temperature dependence of the strain rates at a compression stress of 100 MPa for the PHMS-derived material.

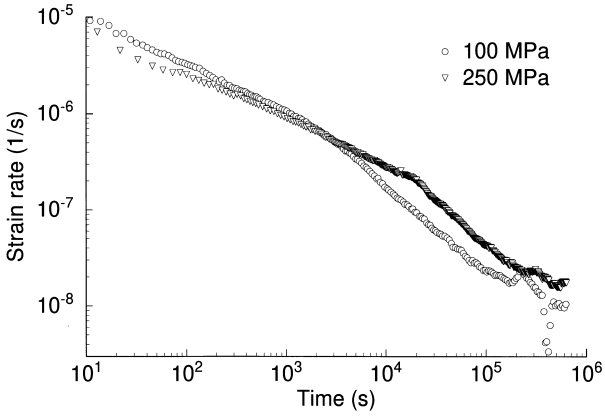

Fig. 5. Stress dependence of the strain rates at 1500°C for the PVS-derived material.

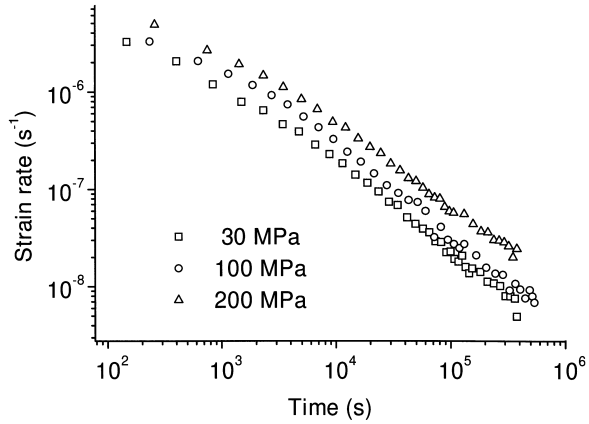

Fig. 7. Stress dependence of the strain rates at 1400°C for the PHMS-derived material.

between creep curves of an as-thermolysed specimen with specimens annealed at 1400°C for different annealing times. A comparison of the strain rates shows that the time exponent of annealed specimens was lower than those of the corresponding as-thermolysed specimens (Fig. 9). The influence of the annealing therefore diminished with testing time.

The reproducibility of the results was a concern, because an intersection of creep curves at different stresses was observed during the experiments, e.g. in Fig. 5. When several specimens were tested under the same conditions, it was observed that initial creep deformation varied somewhat from specimen to specimen, while the long-time creep rates after 100 h creep deformation were reproducible (Fig. 10).

3.2 Oxidation resistance

The oxidation resistance of the two materials was very similar. At temperatures up to 1500°C a dense passivating oxide layer was always found on the surface of the creep specimens. Figure 11 shows a PVS-derived specimen which was tested for 300 h at 1500°C with stepwise increased compression stresses from 100 to 300 MPa. A multiple oxide layer with an overall thickness of 10 μm can be seen. In Fig. 12 the oxidation layer of a PHMS-derived material is shown. After 100 h at 1500°C, the layer had a thickness of 2·2 μm. However, after the creep tests at 1550°C no oxidation layer was found on the surface of both materials, but an area of high porosity near to the surface occurred, indicating a decomposition of the specimens (Figs. 13 and 14).

4 Discussion

The creep deformation of the precursor-derived materials investigated under compression is characterised by rather high initial strain rates. It is assumed that the thermolysis at 1050°C for 4 h is not sufficient to reach a stable ceramic. It was shown with dilatometer experiments that shrinkage of the specimens begins at the thermolysis temperature also in the absence of compression stresses.[15]

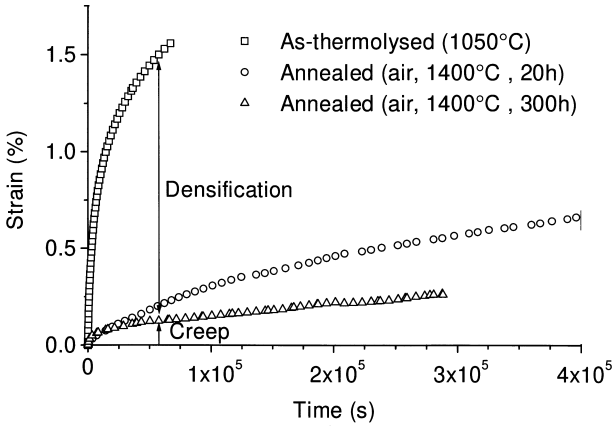

Fig. 8. Influence of different annealing times at 1400°C in air on the creep curves of PVS-derived materials at 1400°C and 100 MPa compression stress.

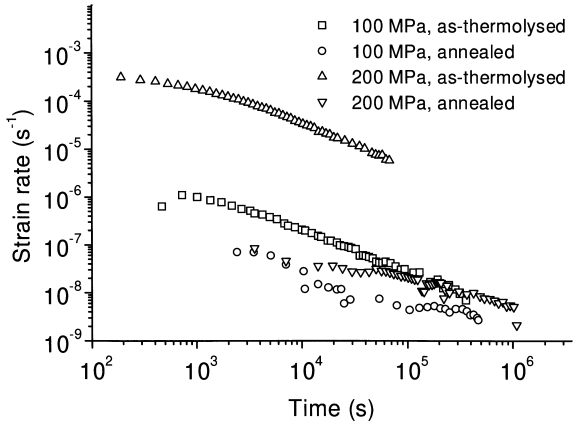

Fig. 9. Influence of 20 h annealing time at 1400°C in air on the creep curves of PHMS-derived material at 1400°C.

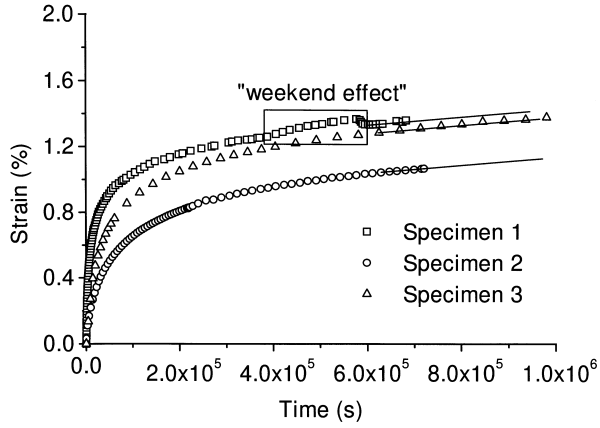

Fig. 10. Variation of creep deformation from specimen to specimen (PVS-derived material, 1400°C, 100 MPa).

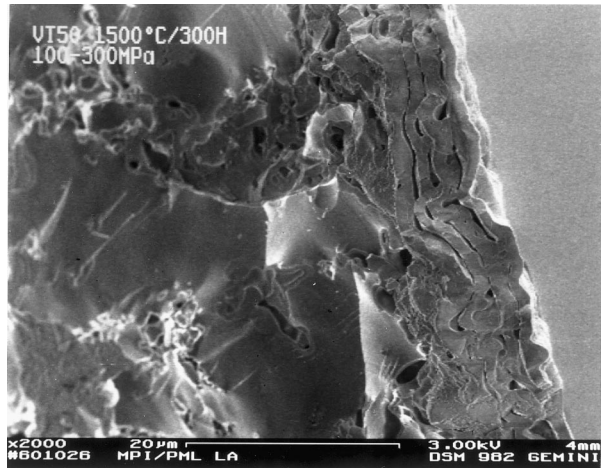

Fig. 11. Fracture surface with oxidation layers of a PVS-derived creep specimen tested for 300 h at 1500°C and compression stresses of 100, 200 and 300 MPa.

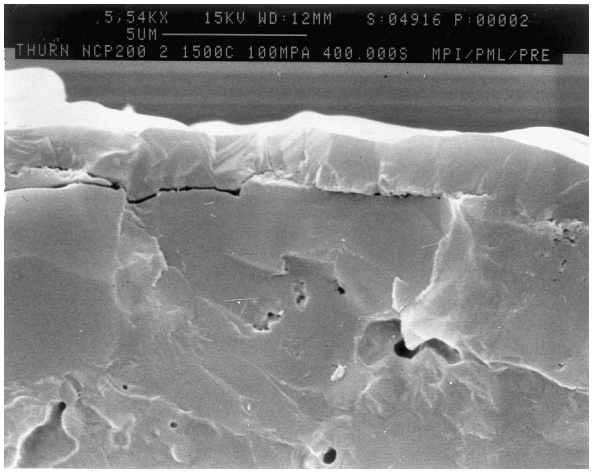

Fig. 12. Fracture surface with oxidation layer of a PHMS-derived creep specimen tested for 100 h at 1500°C and 100 MPa compression stress.

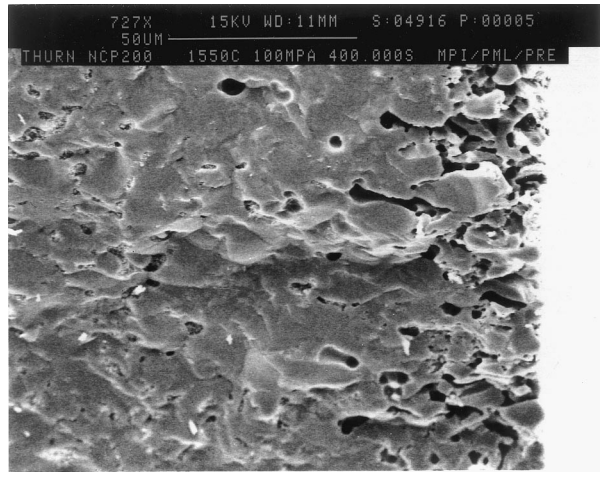

Fig. 14. Fracture surface near the lateral surface of a PHMS-derived creep specimen tested for 100 h at 1550°C and 100 MPa compression stress.

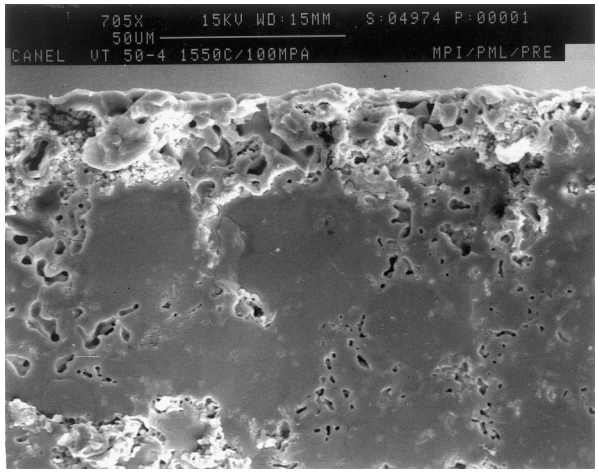

Fig. 13. Fracture surface near the lateral surface of a PVS-derived creep specimen tested for 100 h at 1550°C and 100 MPa compression stress.

Annealing of the specimens has obviously two effects: comparison of polished sections of specimens in the as-thermolysed state and after 20 h heat treatment at 1400°C in air shows a decrease of porosity after annealing. Density measurements on ceramics crushed into very fine powders which are supposed not to contain any porosity indicated an increase of the density of the amorphous matrix to have occurred during creep deformation in addition to a reduction of porosity. The matrix density of PVS-derived material, e.g. increased during annealing from 2·23 g cm^{-3} in the as-thermolysed state to 2·43 g cm^{-3} after $7{\cdot}2\times10^4$ s at 1400°C. A crystalline ceramic with the chemical composition of the PVS-derived material, consisting of silicon nitride with a density of 3·20 g cm^{-3} and graphite with a density of 2·25 g cm^{-3} would have a density of 2·8 g cm^{-3}. From this density the free volume in the amorphous PVS-derived material can be estimated to decrease from 20·4 to 13·2% during annealing. Both the decrease of porosity and the decrease of the molar free volume have an influence on the creep resistance of the material. However from the experimental data the contribution of the two effects cannot be distinguished.

Assuming that the overall strain rates which were measured after $3{\cdot}6\times10^5$ s of creep deformation is a superposition of stress-independent densification and a creep deformation

$$\dot{\varepsilon} = \dot{\varepsilon}(\sigma, T, t) + \dot{\varepsilon}(T, t),$$

the apparent stress exponent calculated from the total deformation is too low and stress dependent. Assuming a stress-independent stress exponent according to the Norton power-law relation, the contribution of shrinkage to the deformation can be estimated to be 74% of the strain rate at 100 MPa compression stress, while the stress exponent of creep deformation is $n = 2.8$. In general viscous flow with a stress exponent $n = 1$ is assumed to be the deformation mechanism in an amorphous solid.[11] The higher stress exponent indicates that other mechanisms may also contribute to the deformation.

It is assumed that the densification rate of the matrix is temperature dependent. Comparison of the strain rates after 100 h of creep deformation revealed a low apparent activation energy. However probably materials with different matrix densities have been compared, so that there is no physical meaning to this apparent activation energy. TEM investigations have been performed to investigate the crystallisation of the materials. No crystalline phases where found after testing at 1400°C and lower temperatures (Fig. 15). However nanosized crystalline Si_3N_4 was found in both the PHMS- and the PVS-derived material after creep tests at 1550°C.[6] This explains the lower strain rates at 1550°C compared to 1500°C.

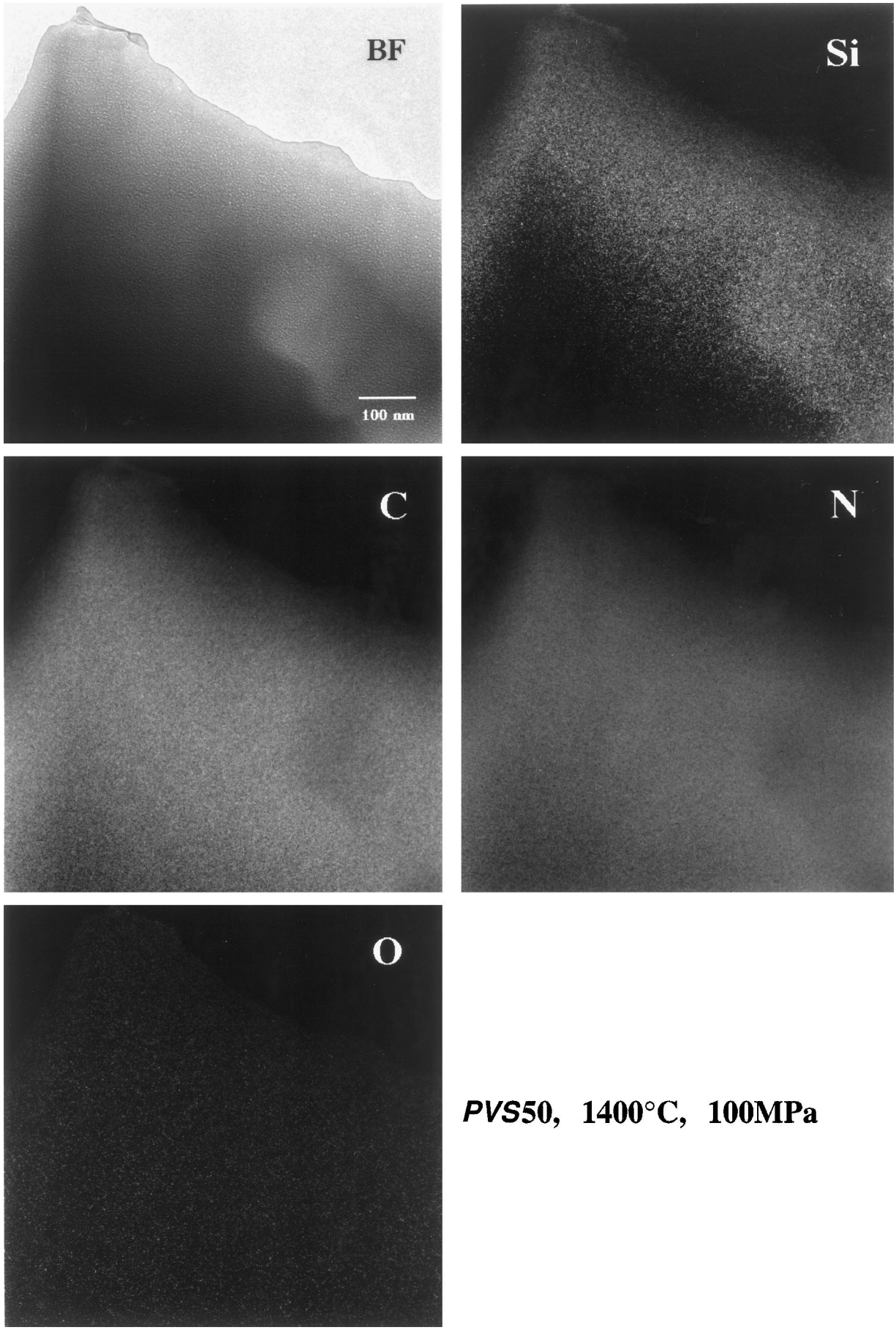

Fig. 15. TEM bright-field image and elemental distribution images of the material obtained from PVS after a creep test at 1400°C with 100 MPa compression stress for 1200 h in air.

It is interesting to note that the total compression strain after 100 h creep deformation under 100 MPa compression stress at 1550°C remained below about 1·4 and 2% for the PVS- and PHMS-derived material, respectively. Since the temperature dependence of the creep deformation revealed a rather low activation energy of 250 kJ mol^{-1} which is only about one-fourth of values typical for liquid-phase-sintered silicon nitride, these results indicate that amorphous precursor-derived materials reveal an interesting potential for high-temperature applications. In liquid phase sintered silicon nitride tensile creep rates are up to two orders of magnitude higher than under compressive loading because of cavitation.[16] As cavitation is suppressed in ceramics without grain boundary phase,[17] the creep resistance of precursor derived ceramic is expected to be superior to silicon nitride under tensile loading.

The oxidation behaviour of the materials investigated is very much controlled by the formation of silica layers at the surface. Since there are no grain boundaries and intergranular oxide-type phases, there is no interdiffusion of oxygen into inner parts of the sample along grain boundary phases being the main oxidation process in liquid-phase-sintered ceramics at high temperatures. In summary one can say that the results show very interesting properties indicating precursor-derived amorphous covalent materials to be a new class of high temperature materials.

Acknowledgements

The authors thank J. Seitz and M. Christ for the production of specimens and the development of experimental methods. TEM investigations were performed by A. Jalowiecki, which is gratefully acknowledged. We also wish to thank the Deutsche Forschungsgemeinschaft DFG and the Japan Science and Technology Corporation (JST) for financial support.

References

1. Bill, J. and Aldinger, F., Precursor-derived covalent ceramics. *Advanced Materials*, 1995, **7**, 775–787.
2. Riedel, R., Kienzle, A., Dressler, W., Ruwisch, L., Bill, J. and Aldinger, F., A siliconboron carbonitride ceramic stable to 2,000°C. *Nature*, 1996, **382**, 796–798.
3. Franke, R., Bender, S., Arzberger, I., Hormes, J., Jansen, M., Jungermann, H. and Löffelholz, J., The determination of local structural units in amorphous SiBN3C by means of X-ray photoelectron and X-ray absorption spectroscopy. *Fresenius J. Analytical Chemistry*, 1996, **354**, 874–878.
4. Seitz, J., Bill, J., Egger, N. and Aldinger, F., Structural investigations of Si/C/N-ceramics from polysilazane precursors by nuclear magnetic resonance. *J. Euro. Ceram. Soc.*, 1996, **16**, 885–891.
5. Dürr, J., Schempp, S., Lamparter, P., Bill, J. and Steeb, S., X-ray and neutron small angle scattering with Si–C–N ceramics using isotopic substitution. *Solid State Ionics*, 1997, **101**, 1041–1047.
6. Bill, J., Seitz, J., Thurn, G., Dürr, J., Canel, J., Janos, B. Z., Jalowiecki, A., Sauter, D., Schempp, S., Lamparter, H. P., Mayer, J. and Aldinger, F., Structure analysis and properties of Si–C–N ceramics derived from polysilazanes. *Phys. Stat. Sol. (a)*, 1998, **166**, 269–296.
7. Schempp, S., Dürr, J., Lamparter, P., Bill, J. and Aldinger, F., Study of the atomic structure and phase separation in amorphous Si–C–N ceramics by X-ray and neutron diffraction. *Z. Naturforsch*, 1998, **53a**, 127–133.
8. Zachariasen, W. H., *J. Am. Chem. Soc.*, 1932, **54**, 3841.
9. Bill, J. and Aldinger, F., Progress in material synthesis. *Z. Metallkd*, 1996, **87**, 827–840.
10. Baufeld, B., Wakai, F. and Honda, S. Mechanical properties of Si–B–C–N precursor derived ceramics. In *Proceedings of the 6th International Symposium on Ceramic Materials and Components for Engines*, ed. K. Niihara, S. Hirano, S. Kanzaki, K. Komeya and K. Morinaga, Arita, 1997, pp. 377–382
11. An, L., Riedel, R., Konetschny, C., Kleebe, H.-J. and Raj, R., Newtonian viscosity of amorphous silicon carbonitride at high temperature. *J. Am. Ceram. Soc.*, 1998, **81**, 1349–1352.
12. Thurn, G. and Aldinger, F., Compression creep behaviour of precursor-derived ceramics. In *Precursor Derived Ceramics*, ed. J. Bill, F. Wakai and F. Aldinger, Wiley VCH, Weinheim, 1999, pp. 237–245.
13. Baufeld B., Gu, H., Bill, J., Wakai, F. and Aldinger F., *J. Euro. Ceram. Soc.*, in press.
14. Seitz, J. and Bill, J., Production of compact polysilazane-derived Si/C/N-ceramics by plastic forming. *J. Mater. Sci. Let.*, 1996, **15**, 391–393.
15. Nishimura, T., Haug, R., Bill, J., Thurn, G. and Aldinger, F., Mechanical and thermal properties of Si–C–N material from polyvinylsilazane. *J. Mater. Sci.*, 1998, **33**, 5237–5241.
16. Luecke, W. E., Wiederhorn, S. M., Hockey, B. J., Krause, R. E. Jr. and Long, G. G., Cavitation contributes substantially to tensile creep in silicon nitride. *J. Am. Ceram. Soc.*, 1995, **78**, 2085–2096.
17. Robertson, A. G., Wilkinson, D. S. and Cáceres, C. H., Creep and creep fracture in hot-pressed alumina. *J. Am. Ceram. Soc.*, 1991, **74**, 915–921.